Received: 5 November 2021 | Revised: 20 February 2022 | Accepted: 4 March 2022

IET Generation, Transmission & Distribution

DOI: 10.1049/gtd2.12470

The Institution of Engineering and Technology WILEY

ORIGINAL RESEARCH

Reliability interdependencies and causality assessment for a converter-penetrated power system

Bowen Zhang | **Mengqi Wang** | **Wencong Su**

Department of Electrical and Computer Engineering, College of Engineering & Computer Science, University of Michigan-Dearborn, Michigan, USA

Correspondence
Mengqi Wang, Department of Electrical and Computer Engineering, College of Engineering & Computer Science, University of Michigan-Dearborn, MI 48128, USA.
Email: mengqiw@umich.edu
Wencong Su, Department of Electrical and Computer Engineering, College of Engineering & Computer Science, University of Michigan-Dearborn, MI 48128, USA.
Email: wencong@umich.edu

Abstract

This paper utilizes Bayesian network (BN) structure searching and scoring algorithms to identify critical nodes and investigate their reliability interdependencies for a power system under great converter penetration. As more converters are integrated into the system, reliability interactions among various converters will frequently emerge and consequently introduce system reliability concerns. However, reliability causal relations have rarely been explored and demonstrated in a clear manner. Therefore, the authors apply BN structure searching and scoring algorithms to visualize the proposed converter-based BN structure. Moreover, reliability interactions among different nodes are quantified through information entropy theory. Numerical case studies illustrate the causal reliability relationship among various nodes while considering the reliability of all integrated converters. Critical nodes are identified such that system operators can improve the converter maintenance scheduling.

1 | INTRODUCTION

With the deepening integration of renewable energy sources (RES), the complexity of evaluating a power system's reliability has been increasing progressively in recent years. Compared with traditional power generation, for example, RESs are easily influenced by ambient conditions. Intermittency of an RES may cause uncertainty issues in system operation and weaken the system's reliability [1–5]. On the other hand, the power electronic converter is essentially integrated and performs the underpinning role of realizing power conversions between RES/battery storage and the main power grid. Moving towards 100% RES integration has further intensified the significance and importance of analyzing the reliability performance of power systems under great converter penetration.

Table 1 provides a brief literature summary on both component and system level reliability analysis. From the component perspective, identifying critical components in a power system has raised much research attention [6–11]. Various components, including transmission lines [6], transformers [7, 8], energy storage systems [9], and load points [10], have been considered most critical when conducting system reliability evaluation. However, converter reliability has rarely been considered as one of the potential causes of system failures in the existing literature. Converter reliability impacts on the overall system reliability have spurred only limited research attention [16, 17]. The authors in [16] considered the power converter one of the most frequently failed components in various applications and thus that increasing converter implementation will have great impact on system reliability performance. A DC–DC converter reliability model was formulated in [9] in evaluating the reliability of an energy storage system, but its impact on other components' reliability was not investigated and different types of converters were not considered. The authors in [17] provided a reliability ranking for multiple converters based on their impacts on system reliability, but the reliability effects/relations among different converters were not explored.

From the system-level perspective, illustrating a system network through a graph that is composed of many nodes with various mutual relations [13] can clearly demonstrate the risk points such that the system reliability can be improved. Today's power system network is clearly amenable to such description. Reference [12] utilized complex network theory to conduct node clustering and visualized the system network augmentation. The authors in [14] investigated various scenarios of system cascading failure, with all failed load points graphically

TABLE 1 Literature summary of component and system level reliability analysis

Research areas	Ref.	Research focus	Consider converter reliability?	Reliability quantification
Component	[6]	Transmission lines	No	Customer interruption cost
	[7, 8]	Transformer	No	EENS
	[9]	Battery systems	Yes (DC–DC converter only)	Failure rate
	[10]	Critical loads	No	Cumulative service time
	[11]	RES	No	Cost of energy
System	[12]	Structural improvement	No	Node clusters
	[13]	Electric/information system interdependency	No	Node coupling rate
	[14, 15]	Cascading failure	No	Failure probability

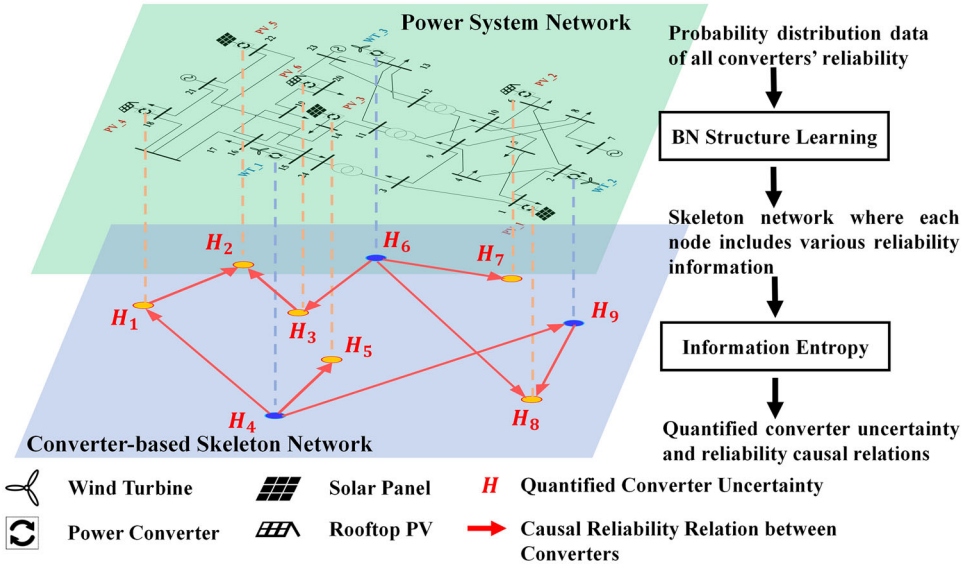

FIGURE 1 An overview of the proposed reliability evaluation framework

presented. In terms of the system reliability correlation, the authors in [13] claimed that there is a clear reliability interdependency between the power system and the information and communication technology (ICT) systems. However, the other type of interaction, namely, the causal relation/connectivity between components has rarely been investigated in the existing literature. A signal directed graph was used in [18] to describe a system with a graphical representation of causal relations amongst variables that can be applied to find fault propagation paths and explain the causes of a fault. However, this method was greatly dependent on human effort and only suitable for linear models. Complex network theory was used in [19] for detecting variable correlations, but its electrical explanation of each node was not straightforward. A more universal approach should be utilized if those interactions and the system itself have strong non-linearity.

This paper mainly focuses on learning the skeleton structure and investigating the causal reliability relations among the integrated converters of a converter-penetrated power system where each converter reliability model is considered. Figure 1 illustrates an overview of the reliability evaluation framework. The proposed electric power system is implemented with multiple renewable energy generators such as wind energy and solar power sources. Specific power converters are integrated with each RES to properly convert the generated renewable power and transfer it to the main grid. As more RESs and converters penetrate the system, it is technically difficult and less efficient to observe the state of every component when evaluating/analyzing the system reliability. However, converters are greatly distributed across the system and as mentioned before, are one of the most vulnerable components/subsystems in a power system. Therefore, we utilize both Bayesian network (BN) [20] structure learning algorithms and information entropy theory [25] to construct a converter-based BN structure where

- Each node considers the reliability of multiple components, including the generator, transformer and especially, the reliability of the converter connected on it. Probabilistic data of each converter's reliability are collected, and we apply Shannon entropy H to quantify the uncertainty of each node.

- Each oriented edge refers to the causal reliability relation between two nodes. The existence of each edge is addressed by calculating mutual information and we determine the edge orientation by calculating transfer entropy such that each causal reliability relation between two nodes can be quantified.
- Those nodes that have high uncertainty and wide influential relations on other nodes are identified as critical to help the system operator optimize schedule prior maintenance/inspections.

It is worth noting that an increasing integration of RES will bring a deep penetration/implementation of power converters in a power system and it is more appropriate to dynamically consider the reliability effect introduced by various types of converters. The generated converter-based BN structure is unique from the original physical power system network. Information such as the level of uncertainty on each node, the quantified causal relations among multiple nodes can only be revealed under the generated BN structure instead of the original physical network. We aim to enhance the importance of considering power converters reliability effects and causal interactions when evaluating the reliability of today's power system. The proposed BN structure demonstrates these focuses and can perform as an evaluation enrichment compared with existing system reliability assessment.

The main contributions of this paper are three-fold

1. This paper proposes a converter-based BN that performs as the skeleton structure of a converter-penetrated power system and utilizes BN structure learning to visualize identified causal relations among different nodes. The reliability of each power converter is enhanced during the learning procedure. As more RESs and energy storage systems are integrated into the system, power converters are heavily distributed and play a very important role in today's power system. Their importance should be further enhanced.
2. This paper for the first time integrates information entropy theory to quantify the uncertainty of each node and each causal relation such that the criticality/vulnerability of all nodes can be provided for system operators to better schedule operations and maintenance.
3. This paper utilizes BN structure learning and transfer entropy estimation methods collaboratively to illustrate comprehensively the causality among various nodes. The reliability interdependency and failure propagation are clearly illustrated to enrich the understanding of the reliability performance of a converter-penetrated power system.

The rest of this paper is organized as follows. First, the concept of BN structure learning and information entropy concepts are presented in Section 2. Section 3 provides the reliability modelling of wind turbines/five photovoltaic (WT/PV) converters and an overview of the proposed system reliability evaluation framework. In Section 4, several case studies are conducted on a modified IEEE 24-bus RTS to demonstrate the effectiveness of the proposed methodology. Conclusions and future works are summarized in Section 5.

2 | TRANSFER ENTROPY-INTEGRATED BN STRUCTURE LEARNING

In this work, BN structure learning and transfer entropy are collaboratively applied to the proposed converter-penetrated power system for investigating the causal relationships among different converter reliability performance. Basic concepts and the proposed transfer entropy-integrated BN structure learning are introduced in this section.

2.1 | Bayesian network structure learning

The BN has been proven to be a versatile tool in various fields [20, 21]. It has been considered one of the most effective and classic graphical models in power system reliability studies as well as providing probabilistic information and inferences via a directed acyclic graph (DAG). The proposed BN structure consists of three components: (V, E, Θ), where a set of nodes $V = \{X_1, X_2, \ldots, X_N\}$ represent N power converters' reliability, and we can assess the reliability of each converter from system Monte Carlo simulation and observe the physical/thermal behaviour of each converter. As more power converters are integrated into the power system, the scale of V will increase; E denotes the set of edges. Each element e_{ij} in E represents an edge directed from X_i to X_j, which represents the causal relation between two converters' reliability performance; Each element $\theta_i \in \Theta$ denotes the conditional probability distributions of the converter reliability X_i.

2.2 | Search and score functions

Currently, search and score-based methods are usually applied to construct BN structures [22, 23]. Search algorithms together with several scoring functions are applied to evaluate the goodness of each explored feasible BN structure. The objective of utilizing this method is to find a DAG that maximizes the selected scoring function. The search algorithm determines the structure learning efficiency while the scoring function affects the learning accuracy.

With a given data set D, the problem of BN structure learning from D can be described as follows: finding a DAG (G) which is the best fit for the data set D in some senses. The scoring function is applied to evaluate the fitness of a candidate DAG to D. The scoring criteria are shown in Equation (1) where the value of $score(D)$ can be determined by the data set D.

$$score\ (G, D) = score(G|D)score\,(D) \tag{1}$$

$$G^* = \arg\max_{G \in G^n} score(G|D) \tag{2}$$

Equation (2) states that the objective is to find the optimal BN structure G^* where G^n is the set of all feasible DAGs.

The BIC scoring function was proposed based on an assumption that samples are subject to independence and an identical distribution. In BIC, the fitness of a DAG for the given data set D is evaluated based on log likelihood. The formula of the BIC scoring function is shown in Equation (3), where N is the number of variables in the DAG; P_i is the number of possible configurations of the parent set $Pa_G(X_i)$ of X_i; S_i is the number of states of the variable X_i; m_{ijk} is the number of observations in the data set D where the variable X_i is under the state k and the parent set is in the jth configuration; $\theta_{ijk} = \frac{m_{ijk}}{m_{ij}}$ $(0 \le \theta_{ijk} \le 1,\ \sum_k \theta_{ijk} = 1,\ m_{ij} = \sum_{k=1}^{r_i} m_{ijk})$ is the likelihood conditional probability; m is the number of samples in D. The first item of this BIC scoring is the log likelihood and the second item performs as a penalty function to avoid overfitting.

$$BIC\ (G|D) = \sum_{i=1}^{X_N}\sum_{j=1}^{P_i}\sum_{k=1}^{S_i} m_{ijk}\log\theta_{ijk} - \frac{1}{2}\sum_{i=1}^{X_N} P_i\,(S_i - 1)\log m \tag{3}$$

Another scoring function named BDe is proposed based on Bayesian statistics and is shown in Equation (4), where $\alpha_{ij} = \sum_{k=1}^{S_i}\alpha_{ijk}$ and α_{ijk} describes the prior distribution. The main principle of BDe is to find a DAG that can maximize the posterior probability considering both data characteristics and prior knowledge.

$$BDe\ (G|D) = \sum_{i=1}^{X_N}\sum_{j=1}^{P_i}\left[\log\frac{\Gamma(\alpha_{ij})}{\Gamma(\alpha_{ij}+m_{ij})} + \sum_{k=1}^{S_i}\log\frac{\Gamma(\alpha_{ijk}+m_{ijk})}{\Gamma(\alpha_{ijk})}\right] \tag{4}$$

In terms of the search algorithm, however, searching the optimal network structure is a non-deterministic polynomial-hard problem. Thus, widely used score-based algorithms, namely K2 and max-min hill-climbing (MMHC) algorithms, are selected as the search strategy.

The K2 algorithm can reduce computational by requiring a prior ordering of nodes as input. The potential parent set of converter X_i can include only those converters that precede it in the given ordering. In the K2 algorithm, the candidate parent nodes set π for X_i are initially set as empty. The algorithm searches π for each X_i according to the specified sequence in the node ordering. The principle of K2 search is to assume that each node is not connected to any parent node at first and then to add parent nodes repeatedly with a given node ordering.

The MMHC algorithm is classified as a combined method, applying concepts and techniques from local learning, search-and-score and constraint-based methods. MMHC first learns the skeleton of a BN structure, namely, the edges without their orientation, using a local discovery algorithm called max-min parents and children (MMPC). MMPC is conducted on all variable pairs and provides a way to identify the existence of each edge. All network edges can be identified by invoking MMPC with each X_i.

2.3 | Transfer entropy

Information entropy is a well-known signal-processing technique, and it has recently proved its suitability for evaluating complex system reliability such as fault detection [24, 27] and uncertainty quantification [25]. The concept of information entropy was proposed as a measure of information and uncertainty of a variable [26, 28]. Suppose there are two variables...' and B and their states (a_j^t, b_k^t) are observed at each hour t. An entropy rate h_1 is defined as the amount of additional information required to represent the value of the next observation of A

$$h_{\mathrm{I}} = -\sum_{j=1}^{S_j}\sum_{k=1}^{S_k} P\left(a_j^{t+1}, a_j^t, b_k^t\right)\log P(a_j^{t+1}|a_j^t, b_k^t) \tag{5}$$

On the other hand, if a_j^{t+1} is independent of the current observation b_k^t, the entropy rate is calculated as in Equation (6):

$$h_{\mathrm{II}} = -\sum_{j=1}^{S_j}\sum_{k=1}^{S_k} P\left(a_j^{t+1}, a_j^t, b_k^t\right)\log P(a_j^{t+1}|a_j^t) \tag{6}$$

In general, the quantity of h_{I} represents the entropy rate when the current state of B can affect the future state of A, while h_2 assumes the future state of A is independent of the current state of B.

Thus, the transfer entropy is defined as the deviation from independence of the state transition of an information destination B from the previous state of an information source A. When the observation delay is 1 h, the transfer entropy can be calculated by (7):

$$T_{A\to B}(j,k) = h_{\mathrm{II}} - h_{\mathrm{I}} = \sum_{j=1}^{S_j}\sum_{k=1}^{S_k} P\left(a_j^{t+1}, a_j^t, b_k^t\right)\Big| \times \log\left(\frac{P(a_j^{t+1}|a_j^t, b_k^t)}{P(a_j^{t+1}|a_j^t)}\right) \tag{7}$$

where t is the time index, a_j^t and b_k^t indicate the jth and kth states of variables A and B at time t, respectively.

It is assumed in both h_{I} and h_{II} that a_j^{t+1} can be influenced by a_j^t (i.e. the future state of A is influenced by its current state). The value of $T_{A\to B}$ quantifies the information difference between 'assume b_k^t can affect a_j^{t+1}' and 'b_k^t is independent from a_j^{t+1}'. In this way, $T_{A\to B}$ indicates the causal relation between A and B. This formulation is a directional and dynamic measure of information transfer from A to B. It shows that the uncertainty changes of a_j^{t+1} between given conditions of b_k^t and unknown b_k^t can be described using transfer entropy. In other words, the information transferred from b_k^t to a_j^{t+1} can be represented by transfer entropy. The transfer entropy formulation is a

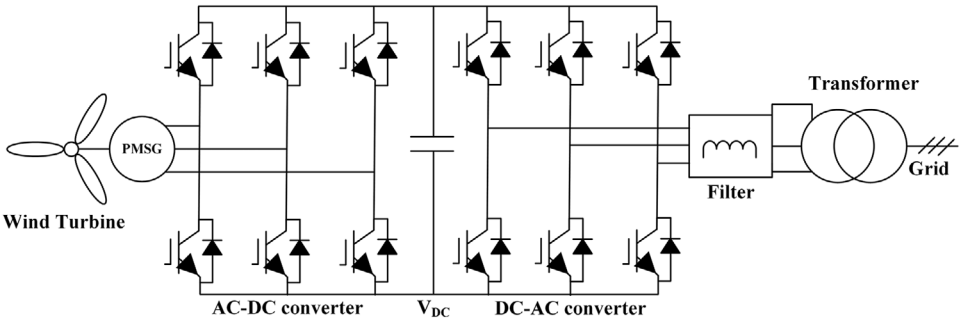

FIGURE 2 A typical converter in a WT power system

generalization of the entropy rate to more than one variable. It is worth noting that transfer entropy remains a measure of the observed correlation rather than of the direct effect between variables.

2.4 | Transfer entropy-integrated scoring function

The causal relations among multiple converters can be complicated since the reliability of each converter can be correlated by many other converters' performance and vice versa. For example, A WT converter failure would terminate the power conversion and the power generated from this WT cannot be transferred into the main grid and also the load side. To supplement power for the affected area, either the battery storage system (BSS) or other available power generations will be required to provide more power compared with their regular power contributions. As a result, this kind of burden will affect the reliability performance of those converters connected with BSS and other renewable generators.

As stated in subsection 2.2, $Pa_G(X_i)$ refers to the parent set of X_i, which means each element in $Pa_G(X_i)$ can potentially affect the reliability of X_i. Thus, multiple edges would exist and all of them would be directed to X_i in the DAG. Moreover, since transfer entropy quantifies the information exchange, it can be utilized as a weighting index on each directed edge and describes the degree of each causal relation. Thus, the total transfer entropy from $Pa_G(X_i)$ to X_i is described in Equation (8), which is used to quantify the reliability causality between each converter X_i and its parent set $Pa_G(X_i)$.

$$T_{Pa_G(Xi)\to X_i}(j,k) = \sum_{j=1}^{S_j}\sum_{k=1}^{S_k} P\left(x_j^{t+1}, x_j^t, Pa_G(X_i)_k^t\right) \Big| \times \log\left(\frac{P(x_j^{t+1}|x_j^t, Pa_G(X_i)_k^t)}{P(x_j^{t+1}|x_j^t)}\right) \quad (8)$$

In terms of the scoring function, as shown in Equation (3), the log likelihood term $(\sum_{i=1}^{N}\sum_{j=1}^{P_i}\sum_{k=1}^{S_i} m_{ijk}\log\theta_{ijk})$ in the BIC scoring function indicates the fitness between the learned DAG and the given data set D, which can be rewritten in Equation (9), where the term within the square bracket represents the entropy when $Pa_G(X_i)$ is given, and can be replaced by h_I in Equation (5). Thus, the log likelihood term in the scoring function can be determined during the transfer entropy calculation

$$\begin{aligned} log\ likelihood\ (G|D) &= \sum_{i=1}^{X_N}\sum_{j=1}^{P_i}\sum_{k=1}^{S_i} m_{ijk}\log\theta_{ijk} \\ &= m\sum_{i=1}^{X_N}\sum_{j=1}^{P_i}\sum_{k=1}^{S_i}\frac{1}{m}m_{ijk}\log\left(\frac{m_{ijk}}{m_{ij}}\right) \\ &= m\sum_{i=1}^{X_N}\left[\sum_{j=1}^{P_i}\sum_{k=1}^{S_i} P(X_i, Pa_G(X_i))\log P(X_i|Pa_G(X_i))\right] \\ &= -mh_I \end{aligned}$$

In general, each transfer entropy value is calculated to quantify the causal relation between each element of $Pa_G(X_i)$ and X_i. The accumulated transfer entropy $T_{Pa_G(Xi)\to X_i}$ which helps to determine the log likelihood function can be calculated after exploring all elements in $Pa_G(X_i)$. The BIC scoring function is then utilized to evaluate the fitness of each feasible structure.

3 | CONVERTER RELIABILITY AND AN OVERVIEW OF THE PROPOSED FRAMEWORK

3.1 | Reliability model of converters

As shown in Figure 2, a typical wind power system consists of a permanent magnet synchronous generator (PMSG), a generator-side inverter, a dc link, and a grid-side inverter. The WT output power is estimated by a set of hourly-based wind speed and angle data throughout a year. Power losses, including switching and conduction loss, are then calculated to derive the failure rate of each device (e.g. diode and IGBT) [17]. Finally, the WT converter reliability $R_{\mathrm{WT_{conv}}}$ can be expressed as in (10), where $\lambda_{w,t}$ represents the failure rate of device w at time t, N_w is the total number of devices in the WT converter.

$$R_{\mathrm{WT_{conv}}}(t) = e^{-\left(\sum_{w=1}^{N_w}\lambda_{w,t}\right)t} \quad (10)$$

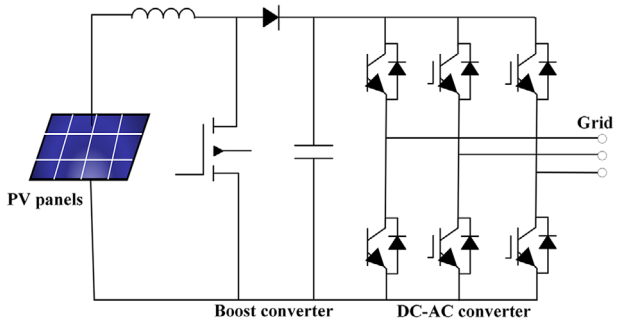

FIGURE 3 A PV system with DC–DC boost and DC–AC inverter

Figure 3 presents a typical PV system considered in this paper which consists of a PV array, a DC–DC boost converter, and a DC–AC inverter. Similarly, hourly-based data, such as solar radiance and ambient temperature, are collected to estimate the PV output power and each device failure rate. Ultimately, the reliability of PV converter $R_{PV_{\text{conv}}}$ can be calculated by (11), where N_p is the total number of devices in the PV converter.

$$R_{PV_{\text{conv}}}(t) = e^{-\left(\sum_{p=1}^{N_p} \lambda_{p,t}\right)t} \tag{11}$$

Since the failure rate is calculated through hourly based data, each component has a failure rate λ at hour t. Meanwhile, the repair rate μ_i is relatively stable and considered a constant. Each component's up and down state probability can be calculated using (12) and (13).

$$P_U(i,t) = \frac{\mu_i}{\lambda_{i,t} + \mu_i} \tag{12}$$

$$P_D(i,t) = \frac{\lambda_{i,t}}{\lambda_{i,t} + \mu_i} \tag{13}$$

3.2 | Reliability of other components

We also consider the reliability of other components such as generators, transformers, transmission lines, and load points. For example, the forced outage rate (FOR), mean time to failure (MTTF), and mean time to recovery (MTTR) are collected for each generator. The detailed reliability data is provided in [32].

3.3 | An overview of the proposed framework

An overview of the proposed reliability evaluation framework is illustrated in Figure 4. In the proposed reliability evaluation framework, the first step is to construct an undirected structure, and a set of training data is required. The data set consists of state vectors $T = \{X_i, \ldots, X_N, L_1, \ldots, L_{tl}, LOLE\}$, where X_i denotes the ith converter reliability. L_i is the state of ith transmission line, and its value equals one if it is under a failed state; otherwise it is zero. $LOLE$ represents the typical reliability indicator, namely, loss of load expectation in the power system. N, tl are the number of integrated converters and transmission lines, respectively. The hourly-based input data such as wind angle, wind speed, ambient temperature, and solar radiance are applied to calculate the reliability of WT/PV converter while reliability data of other components are also collected. State sampling of Monte Carlo simulation [22] is used to determine the state of each component in the system. We summarize the steps of generating the training data as follows: First, the reliability state of each component is determined by generating uniformly distributed random numbers between 0 and 1, which is further compared with the component reliability or FOR. If the sampled value is smaller than the FOR value, the component is under an outage state. Otherwise, the component is under a normal state. After all components' states are determined, the overall system can be under a normal/contingency state and the value of $LOLE$ can be calculated. As introduced in Section 2, BN structure searching algorithms and scoring functions are applied to generate a BN from the original electrical network.

Meanwhile, given the probability distribution of each converter reliability, the Shannon entropy $H(X_i)$ can be calculated to quantify the uncertainty level of each X_i. Based on the training data and expert knowledge, values of mutual information are calculated to determine the existence of edges in the structure.

To investigate the causal relation between converter reliabilities, transfer entropy is further calculated on each edge. It is worth noting that both $T_{X\to Y}$ and $T_{Y\to X}$ should be calculated in terms of variables X and Y. In general, it is asymmetry between $T_{X\to Y}$ and $T_{Y\to X}$. If $T_{X\to Y} \gg T_{Y\to X}$, then the causal relation is considered as $X \to Y$, which means that given the information of X will greatly help predict the reliability performance of Y at that moment, and vice versa. Even X and Y are greatly coupled in reality and they affect each other throughout a year. At a certain time t, however, the causal relation is considered uni-directional if the values of $T_{X\to Y}$ and $T_{Y\to X}$ are not equal.

Since $H(X)$ denotes the uncertainty of each converter and TE explores all causal relations among all converters, a reliability criticality of converters can be generated by comprehensive comparison/analysis of these entropy values. The vulnerability/criticality of each converter is then determined. Identified critical converters should have priority to have maintenance or get equipped with a reliability sensor such that their reliability information can be fully observed/monitored. The overall system entropy, i.e. the system uncertainty, is further reduced.

4 | NUMERICAL ANALYSIS

In this section, the proposed reliability evaluation framework is validated on the modified 24-bus IEEE reliability test system (RTS). The computations, including MC simulations, are performed in Matlab 2020a on an Intel Core at 2.90 GHz with 16 GB RAM. BN structure learning is realized through Bayes Net Toolbox [29] and Python pgmpy [30]. A Matlab toolbox called cTE [31] is modified for the transfer entropy estimations.

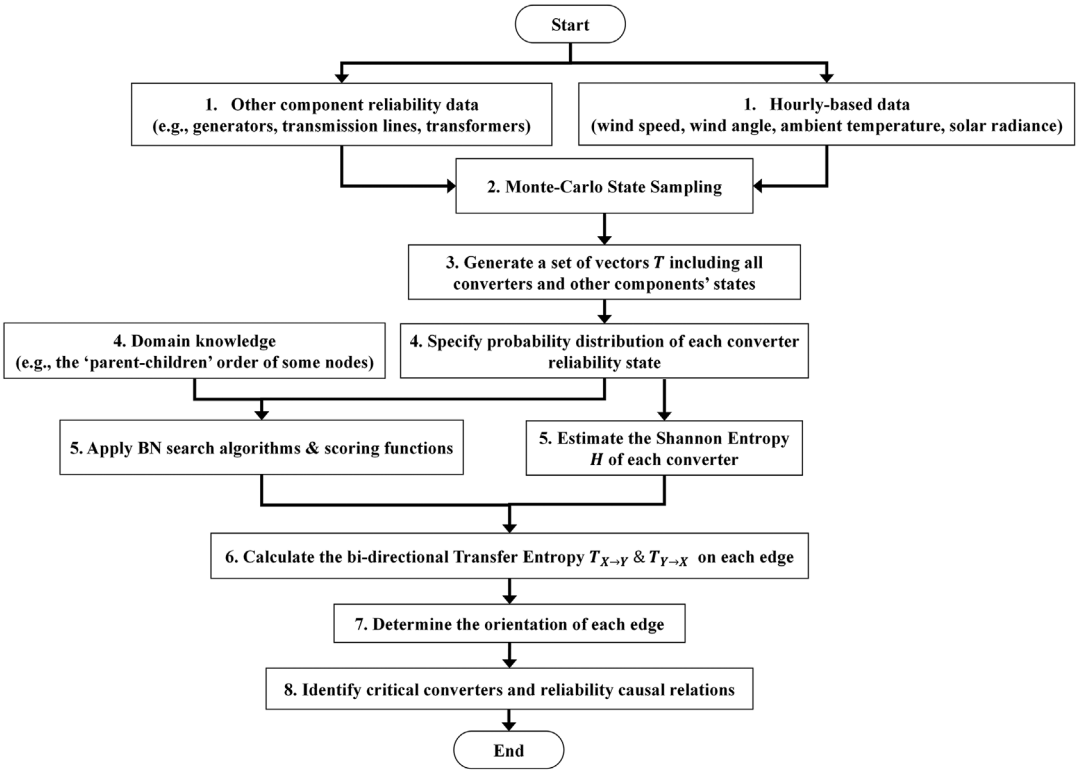

FIGURE 4 An overview of the proposed framework

TABLE 2 Location and capacity information for WT converters

No. of WT	Bus ID	Capacity (MW)
1	1	148.3
2	21	217.5
3	15	155.0
4	7	191.1

TABLE 3 Location and capacity information for PV converters

No. of PV	Bus ID	Capacity (MW)
1	23	51.6
2	14	51.6
3	13	92.7
4	24	49.7
5	22	51.7

4.1 | The modified 24-bus IEEE RTS

Figure 5 presents the modified 24-bus IEEE RTS network. RTS was first published in 1979 as a benchmark for testing various reliability analysis methods. In all case studies, we use the updated version of RTS data [32] where some conventional oil-fueled generating units were replaced by RESs and energy storage systems. Four WT, PV generators and seven rooftop PVs (RFPV) have been added to the system. Tables 2, 3 and 4 provide all RES locations and capacity information.

TABLE 4 Location and capacity information for RFPV converters

No. of RFPV	Bus ID	Capacity (MW)
1	4	27.0
2	5	28.2
3	6	9.7
4	8	11.2
5	19	10.3
6	18	27.2
7	3	9.4

4.2 | BN structure learning based on the transfer entropy-integrated scoring function

As introduced in Sections 1 and 2, the Shannon entropy represents the level of uncertainty on each variable and transfer entropy quantifies the information transferred between two variables. Since each converter reliability performs as a variable, and any converter reliability performance can be passively affected by or can affect other converters, we not only

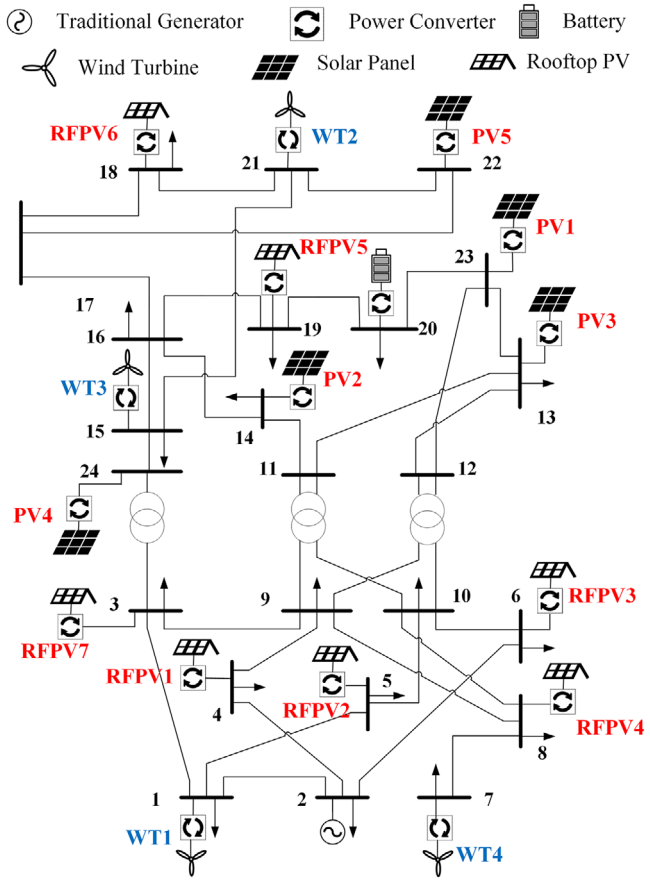

FIGURE 5 The modified 24-bus IEEE RTS network

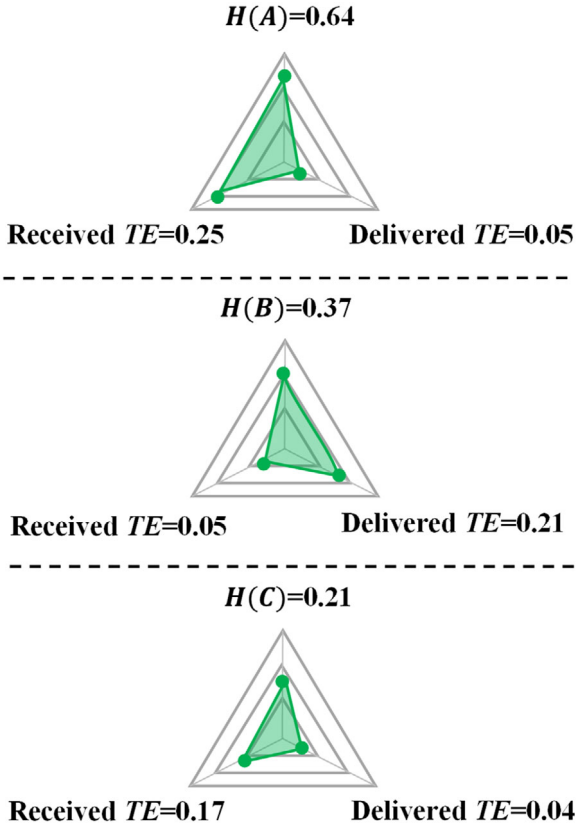

FIGURE 6 Calculated entropy values of each variable

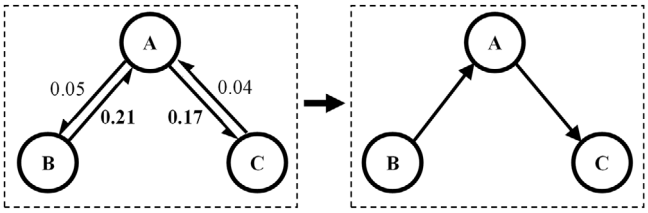

FIGURE 7 An example of determining the edge orientation

TABLE 5 Learning comparisons among different scoring functions

Causal relations	1 → 2	6 → 10	7 → 8	21 → 18
BDe	Y	N	Y	N
BIC	Y	Y	Y	N
Transfer entropy-integrated BIC	Y	Y	Y	Y

estimate the Shannon entropy but also calculate the value of delivered and received transfer entropy of each converter to comprehensively evaluate its importance/criticality. Once the uncertainty of each node and information transferred between two nodes are determined, critical nodes can be identified afterwards.

For example, as shown in Figure 6, in a network with three variables $\{A, B, C\}$, we consider the Shannon entropy of all variables $\{H(A), H(B), H(C)\}$ to quantify the level uncertainty of each variable. Since each variable x will normally deliver/receive some information to/from another variable y, namely, both $T_{x\to y}$ and $T_{y\to x}$ will exist. But their values can be significantly different, which helps quantify the amount of information that x delivered and received. We also calculate these two transfer entropy values to determine the orientation of each causal relation. As shown in Figure 7, since the variable B delivers more information to A and does not receive much information from A, we can conclude that the variable B tends to affect A rather than gets influenced by it. Therefore, the edge orientation between A and B is $B \to A$.

In the proposed network, some causal relations (e.g. node $1 \to 2$, $6 \to 10$, $7 \to 8$ and $21 \to 18$) are obvious by applying prior knowledge. The learning results based on integrated three scoring functions of these assumptions are listed in Table 5. 'Y' indicates that the causal relation between two nodes is correctly learned while 'N' indicates the causal relation is not learned/considered not significant. The proposed function learned all four causal relations correctly while one or two relations were not detected by BIC and BDe, respectively.

Figure 8 presents the BN structure learned from the original 24-bus electrical network, where each node represents the bus reliability, considering the reliability of generator, integrated converter, load and other components, and each directed edge represents the reliability causal relation between two nodes. K2 and MMHC algorithm are applied as the searching strategies to

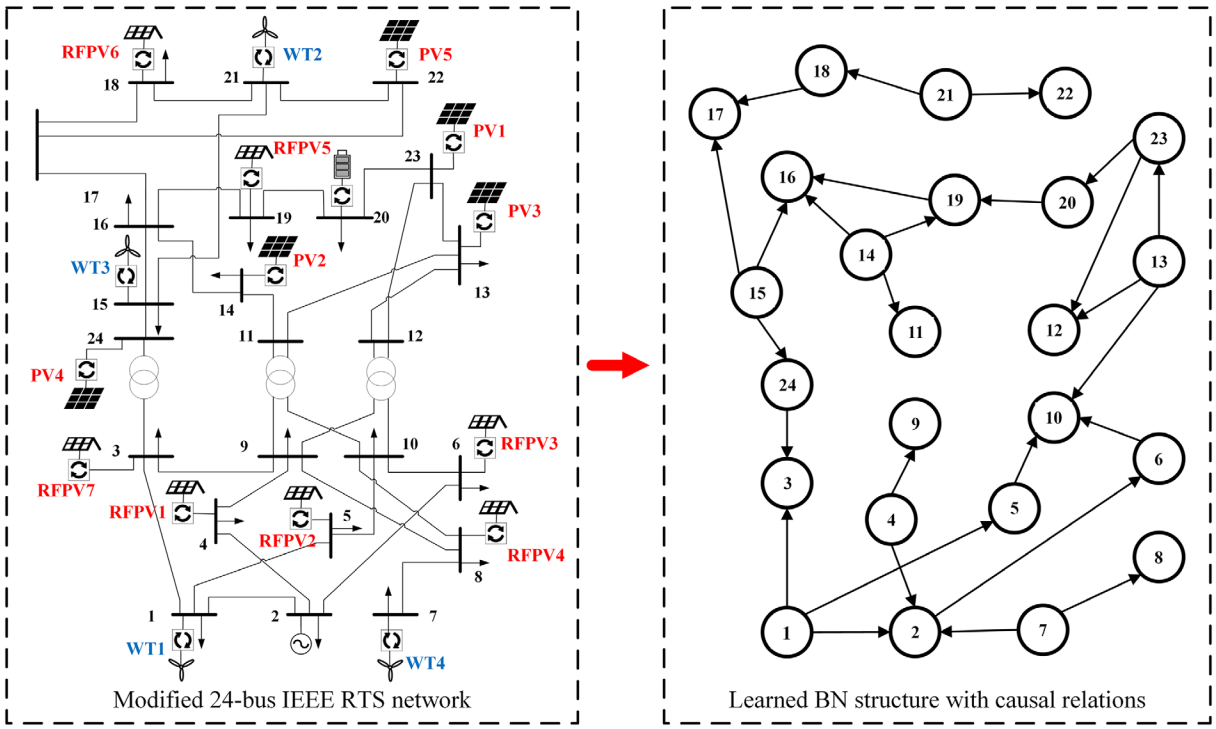

FIGURE 8 The learned BN structure based on the proposed scoring function. (Left figure: Node—bus, edge—physical connection Right figure: Node—reliability of each bus, edge—causal relation). (Note: It is not a one-to-one mapping between the original physical RTS network and the learned BN structure. It is worth noting that this is a one-to-one mapping between the original physical network and the learned BN structure. For example, there exists a physical connection between nodes 9 and 11, but in the learned BN structure, there is no causal relation between these two nodes.) BN, Bayesian network; RTS, reliability test system

explore the BN structure. Prior knowledge such as bus generation and load information, converter FOR [32, 33], and MC simulation data is used to help generate a set of node orders. To avoid structure overfitting and remove weak connections, the threshold value of mutual information is adjusted to 0.10. It can be observed that most nodes have multiple causal relations (edges). For example, node 5 has two edges which indicate its reliability performance can potentially affect the performance of node 10 and can be influenced by the reliability performance of node 1.

Critical nodes are marked with solid red such as {1, 13, 14, 15} in Figure 9 because all orientations of their edges target towards other nodes, which indicate these nodes can deliver more information to other nodes and their reliability can potentially affect the reliability performance on their related nodes. Another set of nodes with red diagonal stripes (e.g. nodes 10 and 16) only have edges pointing towards themselves, which indicate that these nodes can be easily influenced. These nodes receive more information than deliver it such that the reliability on these nodes can be greatly affected by the reliability performance of other nodes. Thus, they are considered as vulnerable compared with the former solid red nodes.

Figure 10 illustrates the calculated entropy values of critical nodes. The Shannon entropy H on nodes 1, 13, 14 and 15 is relatively high which indicates the uncertainty on these nodes is under a high level. The delivered transfer entropy indicates how much information is delivered to other related nodes. Therefore, these nodes are considered more impactful/critical, and moreover, all their edges direct towards other nodes, namely, their reliability performance will probably impact multiple other nodes.

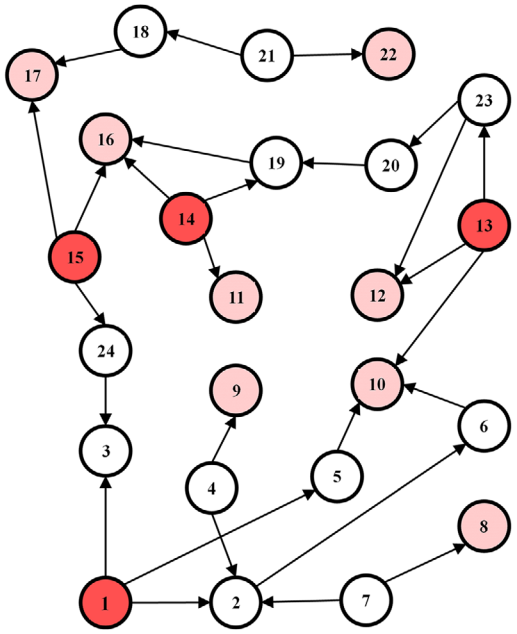

FIGURE 9 Illustrated critical nodes in the BN structure

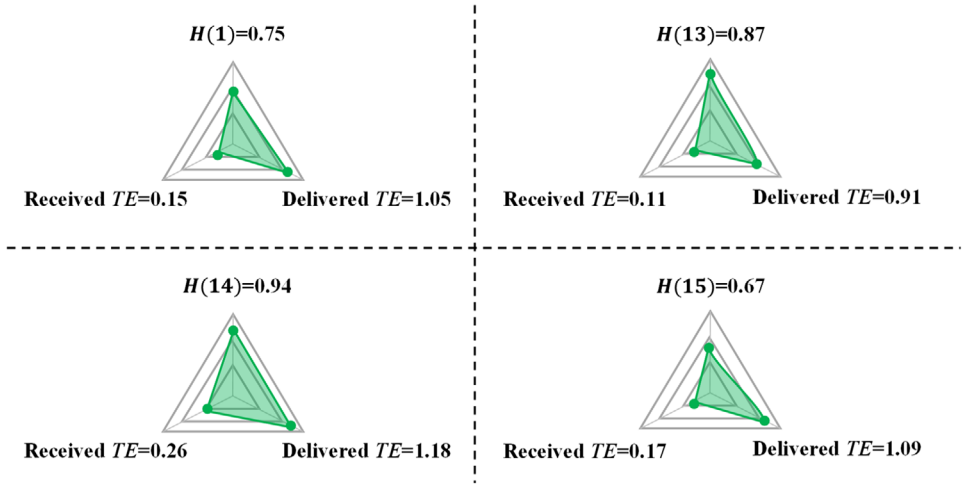

FIGURE 10 Calculated Shannon and transfer entropy (TE) on critical nodes

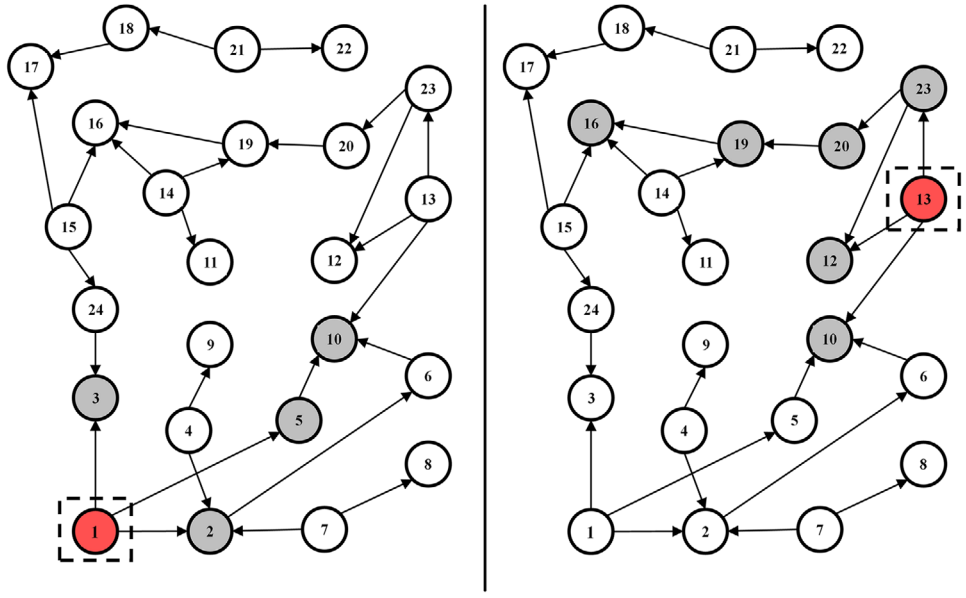

FIGURE 11 The failure propagation area when outage happened on nodes 1 and 13

4.3 | Outages on critical nodes and their propagation areas

Critical nodes such as 1, 13, 14, 15 are identified in the previous subsection and they are more likely to impact the reliability of other nodes. For example, if a converter failure happened on node 1, the performance of nodes 2, 3 and 5 will probably be influenced. However, this does not guarantee that the outage area is limited to these four nodes since nodes {2, 3, 5} also have causal relations with other nodes. Similarly, node 10, for example, can be easily influenced but not limited to {5, 6, 13} since cascading failure can possibly happen.

Node sensitivity refers to how the reliability degree of other nodes is influenced if one node reliability has a small change. The sensitivity analysis is conducted on each critical node and the largest propagation area is presented in Figures 11 and 12. The dotted square on the node indicates a small reliability change is applied while the grey marks the influenced nodes. For example, a small increase on the failure rate of node 13 will increase the outage probability on nodes {10, 12, 23, 20, 19, 16}. It can be observed that the identified causal relations basically match with the failure propagation area and either node 10 or 16 is affected in all analyzed results.

It is worth noting that the learned BN structure is generated and different from the original 24-bus electrical network. The electrical network shows the physical connections while the BN structure illustrates the reliability causal relations among nodes. Since each node uncertainty is quantified by Shannon entropy (the level of uncertainty) and each causal relation is evaluated by transfer entropy, namely, the reliability information transferred

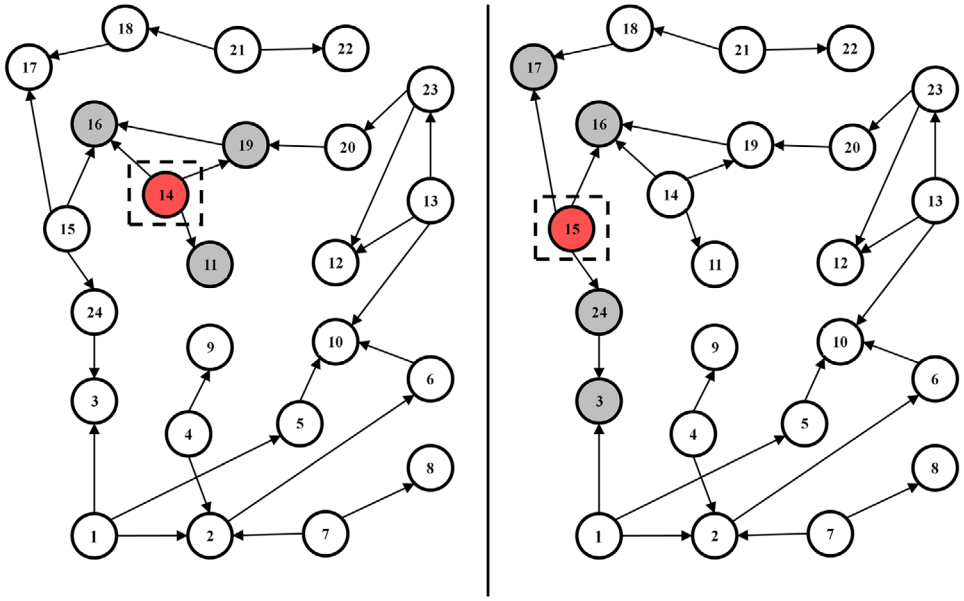

FIGURE 12 The failure propagation area when outage happened on nodes 14 and 15

between nodes, the failure propagation includes events such as cyber-attacks. Therefore, these analyzed propagation areas and quantified uncertainty information cannot be revealed by the original electrical network but are uniquely generated from the BN structure.

5 | CONCLUSIONS AND FUTURE WORKS

This paper has presented a framework to enhance the reliability analysis of a converter-penetrated power system. A BN structure is generated by utilizing BN structure search and scoring algorithms, which can be beneficial for illustrating the causal relations in complex system structures. Not only the uncertainty of each converter, but also various reliability causal relations among converters are explored and quantified through information entropy. Numerical analysis has demonstrated the reliability causal relations among different nodes and has evaluated the criticality/vulnerability of all nodes for system operators to improve the maintenance scheduling. Future research will focus on improving computational costs of complex system BN structure learning. Moreover, the effect of practical node locations, the quality of delivered/received information and their specific impacts can be considered to comprehensively identify critical nodes in the system. An optimal placement or redundancy maintenance strategy can be investigated given a limited number of reliability sensors.

ACKNOWLEDGEMENT

The authors would like to thank the anonymous editor and reviewers for their valuable comments and suggestions to improve the quality of this paper.

FUNDING INFORMATION

N/A

DATA AVAILABILITY STATEMENT

The authors elect to not share data.

CONFLICT OF INTEREST

The authors declare that they have no known competing financial interests or personal relationships that could have appeared to influence the work reported in this paper.

ORCID

Wencong Su https://orcid.org/0000-0003-1482-3078

REFERENCES

1. Hakimi, S.M., Moghaddas-Tafreshi, S.M.: Optimal planning of a smart microgrid including demand response and intermittent renewable energy resources. IEEE Trans. Smart Grid 5(6), 2889–2900 (2014)
2. Su, W., Wang, J., Roh, J.: Stochastic energy scheduling in microgrids with intermittent renewable energy resources. IEEE Trans. Smart Grid 5(4), 1876–1883 (2013)
3. Pourbabak, H., Chen, T., Zhang, B., Su, W.: Control and energy management systems in microgrids. In: Obara, S. (ed.) Clean Energy Microgrids. The Institution of Engineering and Technology (IET) (2017)
4. Su, W., Wang, J.: Energy management systems in microgrid operations. Electri. J. 25(8), 45–60 (2012)
5. Aflaki, S., Netessine, S.: Strategic investment in renewable energy sources: The effect of supply intermittency. Manuf. Service Oper. Manage. 19(3), 489–507 (2017)
6. Hamoud, G.A.: Assessment of transmission system component criticality in the de-regulated electricity market. In: Proceedings of the 10th IEEE International Conference on Probablistic Methods Applied to Power Systems, pp. 1–8. (2008, May)
7. Awadallah, S.K., Milanović, J.V., Jarman, P.N.: The influence of modeling transformer age related failures on system reliability. IEEE Trans. Power Syst. 30(2), 970–979 (2014)

8. Awadallah, S.K., Milanović, J.V., Jarman, P.N.: Quantification of uncertainty in end-of-life failure models of power transformers for transmission systems reliability studies. IEEE Trans. Power Syst. 31(5), 4047–4056 (2015)
9. Liu, M., Li, W., Wang, C., Polis, M.P., Li, J.: Reliability evaluation of large-scale battery energy storage systems. IEEE Trans. Smart Grid 8(6), 2733–2743 (2016)
10. Xu, Y., Liu, C.C., Schneider, K.P., Tuffner, F.K., Ton, D.T.: Microgrids for service restoration to critical load in a resilient distribution system. IEEE Trans. Smart Grid 9(1), 426–437 (2016)
11. Blaabjerg, F., Yang, Y., Ma, K., Wang, X.: Power electronics-the key technology for renewable energy system integration. In 2015 IEEE International Conference on Renewable Energy Research and Applications (ICRERA), pp. 1618–1626. (2015, November)
12. Wang, J., Yu, X., Stone, L.: Effective augmentation of complex networks. Sci. Rep. 6(1), 1–9 (2016)
13. Tøndel, I.A., Foros, J., Kilskar, S.S., Hokstad, P., Jaatun, M.G.: Interdependencies and reliability in the combined ICT and power system: An overview of current research. Appl. Compu. Inform. 14(1), 17–27 (2018)
14. Thapa, M., Espejo-Uribe, J., Pournaras, E.: Measuring network reliability and repairability against cascading failures. J. Intell. Inform. Syst. 52(3), 573–594 (2019)
15. Dong, H., Cui, L.: System reliability under cascading failure models. IEEE Trans. Reliab. 65(2), 929–940 (2015)
16. Peyghami, S., Wang, Z., Blaabjerg, F.: A guideline for reliability prediction in power electronic converters. IEEE Trans. Power Electron. 35(10), 10958–10968 (2020)
17. B. Zhang, M. Wang, W. Su: Reliability analysis of power systems integrated with high-penetration of power converters. IEEE Trans. Power Syst. 36(3), 1998–2009 (2021)
18. Dong, C., Zhao, Y., Zhang, Q.: Assessing the influence of an individual event in complex fault spreading network based on dynamic uncertain causality graph. IEEE Trans. Neural Netw. Learn. Syst. 27(8), 1615–1630 (2016)
19. Saleh, M., Esa, Y., Mohamed, A.: Applications of complex network analysis in electric power systems. Energies 11(6), 1381 (2018)
20. Daemi, T., Ebrahimi, A., Fotuhi-Firuzabad, M.: Constructing the Bayesian network for components reliability importance ranking in composite power systems. Int. J. Electri. Power Energy Syst. 43(1), 474–480 (2012)
21. Shi, Q., Liang, S., Fei, W., Shi, Y., Shi, R.: Study on Bayesian network parameters learning of power system component fault diagnosis based on particle swarm optimization. Int. J. Smart Grid Clean Energy 2(1), 132–137 (2013)
22. Chen, X.W., Anantha, G., Lin, X.: Improving Bayesian network structure learning with mutual information-based node ordering in the K2 algorithm. IEEE Trans. Knowl. Data Eng. 20(5), 628–640 (2008)
23. Tsamardinos, I., Brown, L.E., Aliferis, C.F.: The max-min hill-climbing Bayesian network structure learning algorithm. Mach. Learn. 65(1), 31–78 (2006)
24. Fu, L., He, Z.Y., Mai, R.K., Bo, Z.Q.: Approximate entropy and its application to fault detection and identification in power swing. In 2009 IEEE Power & Energy Society General Meeting, pp. 1–8. (2009, July)
25. Namdari, A., Li, Z.: A review of entropy measures for uncertainty quantification of stochastic processes. Adv. Mech. Eng. 11(6), 1687814019857350 (2019)
26. Schreiber, T.: Measuring information transfer. Phys. Rev. Lett. 85(2), 461 (2000)
27. Kong, L., Pan, H., Li, X., Ma, S., Xu, Q., Zhou, K.: An information entropy-based modeling method for the measurement system. Entropy 21(7), 691 (2019)
28. Shannon, C.E.: A mathematical theory of communication. ACM SIGMOBILE Mobilecomputing Commun. Rev. 5(1), 3–55 (2001)
29. Holmes, D.E. (ed.): Innovations in Bayesian Networks: Theory and Applications, vol. 156. Springer, New York (2008)
30. Ankan, A., Panda, A.: pgmpy: Probabilistic graphical models using python. In: Proceedings of the 14th Python in Science Conference (SCIPY 2015). Citeseer, vol. 10 (2015)
31. Faes, L., Nollo, G., Porta, A.: Information-based detection of nonlinear Granger causality in multivariate processes via a nonuniform embedding technique. Phys. Rev. E 83(5), 051112 (2011)
32. Barrows, C., Bloom, A., Ehlen, A., Ikäheimo, J., Jorgenson, J., Krishnamurthy, D., Lau, J., McBennett, B., O'Connell, M., Preston, E., Staid, A.: The IEEE reliability test system: A proposed 2019 update. IEEE Trans. Power Syst. 35(1), 119–127 (2019)
33. Grigg, C., Wong, P., Albrecht, P., Allan, R., Bhavaraju, M., Billinton, R., Chen, Q., Fong, C., Haddad, S., Kuruganty, S., Li, W.: The IEEE reliability test system-1996. IEEE Trans. Power Syst. 14(3), 1010–1020 (1999)

How to cite this article: Zhang, B., Wang, M., Su, W.: Reliability interdependencies and causality assessment for a converter-penetrated power system. IET Gener. Transm. Distrib. 16, 2547–2558 (2022). https://doi.org/10.1049/gtd2.12470